Sub retrograde geosynchronous orbit SAR: parameter design and performance analysis

Caipin Li, Qingjun Zhang, Jiao Liu, Guoqiang Han, Bo Liu, Chongdi Duan and Zheng Lu

***Abstract*—In recent years, Geosynchronous synthetic aperture radar (GEO SAR) has attracted many scientists to carry out relevant research. Its research is in-depth and gradually maturing. However, conventional GEO SAR has the problems of great influence by the earth's rotation, complex timing design, uneven flight speed in the whole orbit, and non orthogonal range and azimuth resolution, which limits it's application. A new concept of sub retrograde geosynchronous orbit SAR is proposed in this paper. Compared with traditional GEO SAR, the satellite has the advantages of less influence by the earth's rotation, simple timing, uniform motion speed in the whole orbit, shorter revisit time, better resolution and small space-variant in azimuth and range. The radar parameters of sub retrograde GEO SAR are designed. Through the research, it is found that the system sensitivity and resolution no longer change with the orbit position, and its timing design does not need to consider the range migration variation. In addition, the imaging characteristics of sub retrograde GEOSAR are investigated. The results show that, the range model can meet the imaging requirements as long as it is expanded to the fourth order. After that, the influence of orbit perturbation error in sub retrograde GEO SAR is given for the first time. Last, two ways to solve observation blind area of sub retrograde GEO SAR are proposed, one is to change the orbit inclination, another way is to use the bistatic mode.**

***Index Terms*—sub retrograde orbit, geosynchronous synthetic aperture radar (GEO SAR), system parameter design, performance analysis.**

I. Introduction

SINCE geosynchronous orbit synthetic aperture radar (GEO SAR) was proposed, it has attracted the attention of many researchers because of its short revisit period and wide observation swath. Scientists from the United States, China, Britain, Germany, Italy and other countries have carried out research on system design and imaging algorithms. In 1978, K. Tomiyasu first proposed the concept of GEO SAR [1], with the support of National Aeronautics and Space Administration (NASA), the parameter analysis of GEO SAR was carried out. In 1983, with the support of NASA, K. Tomiyasu *et al.*improved the system parameters. It is assumed that the U.S. territory imaged on the geosynchronous orbit with an orbital inclination of 50° and a bisector of 97° west longitude [2]. Then in 1987, Lesley M. from Royal College of Aeronautics also conducted relevant research on the concept, reliability, application and system design of high orbit SAR [3].

In 2003, Jet Propulsion Laboratory (JPL) gave the global seismic satellite system (GESS) scheme [4]-[6], which plans to launch 10 high orbit SAR satellites in 20 years to form an uninterrupted global coverage. German Aerospace Center (DLR) [7] proposed a GEO - LEO SAR conceptual system with separate transceiver. The system uses a geostationary satellite (35850 km) as the launch source and receives it through several formation flying LEO satellites (400 km).

In 2006, I. G. Osipov proposed a GEO SAR system using nuclear fuel as energy [8]. The system is composed of several satellites in LEO, GEO and geostationary orbit, forming a bistatic imaging mode. In 2007, Cranfield University in the UK envisaged using 12 satellites to form a system [9], which was divided into three groups, respectively responsible for three regions: America, Europe and Africa, Asia and Oceania.

In 2012, with the support of ESA, Italy [10] proposed to use 1.4 m small aperture reflector antenna to realize C-band 200 m resolution earth observation. Polytechnic University of Milan and Polytechnic University of Catalonia mainly carried out joint research on GEO SAR system with near zero orbital inclination [11]-[16]. Professor Andrea Monti Guarnieri led the European Space Agency (ESA) GEO SAR for terrain and atmosphere with short review [17]-[22].

In 2014, Hobbs *et al.*outlined the potential application fields and described the main factors restricting its development [23]-[26]. In the same year, Ruiz-Rodon *et al.* analyzed the beam surface coverage of GEO SAR in the case of geostationary orbit and low eccentricity, and verified through simulation that the imaging effect of the system in the mid latitude area is better under its set parameters [27], [28]. In 2015, Andrea Monti Guarnieri *et al.* in Italy put forward the concept of multiple input multiple output (MIMO) GEO SAR. The system uses multiple small satellites in the same frequency band to form a constellation group. Compared with monostatic GEO SAR, it has higher resolution, longer observation time and higher system reliability [28]- [30]. In the same year, Mark E. Davis studied the topographic mapping ability of GEO SAR under the shelter of plants [31]. In 2016, Hans Martin *et al.* put forward the design idea of daily monitoring of the whole Mediterranean region by using GEO SAR. It is demonstrated that the system can be realized based on today's scientific and technological level [32].

Manuscript received xx; revised xx ; accepted xx. Date of publication xx; date of current version xx.This work was supported in part by the National Key Research and Development Program of China under Grant 2022YFB3902404. *(Corresponding author: Qingjun Zhang).*

Caipin Li, Jiao Liu, Guoqiang Han, Bo Liu and Chongdi Duan are with the Xi'an Institute of Space Radio Technology,Weiqu Road,Changan District,Xi'an, China (e-mail: licaipin2010@ 163.com, liujiao70@qq.com, hgqfyw@163.com, liub@cast504.com, duancd@cast504.com).

Qingjun Zhang and Zheng Lu are with China Academy of Space Technology, Institute of Remote Sensing Satellite, No.104, Youyi Road, Haidian District.Beijing, China. (e-mail: ztzhangqj@163.com, lvzheng_cast@163.com).

Color versions of one or more of the figures in this article are available online at http://ieeexplore.ieee.org

In 2019, H Xu *et al.* proposes a SAR system mounted on a special satellite in reverse equatorial geosynchronous orbit, which the orbital inclination of satellites are180°, but there is a risk of collision with satellites in existing orbits [33]. In 2020, C Hu *et al.* proposes an analytical analysis method for the multistatic GEO SAR GAF-based on the array spatial ambiguity function (ASAF) [34], and proposes Coherence based synthetic aperture radar (SAR) tomography (TomoSAR), that exploits the complex coherences of SAR images to achieve 3-D imaging [35]. In 2020, Z Chen *et al*. reviews the research progress of GEO SAR technologies in detail [36]. In 2021, B Zhou *et al.* Proposed a generalized method for calculating the accurate propagation distance between a GEO satellite and a target with ultralong integration time [34]. F Chang *et al.* focus on the analysis of the elevation space-variant error and proposed an imaging algorithm to solve the 3D space variation and improve the focusing depth [38].

Although the research is in-depth, some countries even put forward plans to launch GEO SAR satellites. For example, the G-CLASS Hydroterra project which will be finalized by many famous research institutes, and would carry a synthetic aperture radar and would be rather uniquely placed in a geosynchronous orbit. the project will be launched in 2027-2028 [39]-[41]. With the support of space infrastructure, China is also carrying out key technology research of GEO SAR [42]-[47]. The first GEO SAR has been launched by China at August 2023.

Current GEO is known as inclined anterograde orbit (with an inclination of 0~90°), instead, this paper proposes a concept of retrograde GEO SAR with an inclination of 180°. Considering that if its orbital height is the same as the geostationary orbit, there is a risk of collision with existing satellites. Therefore, we propose the SAR with an orbit height lower than the existing geostationary orbit, which is called sub retrograde GEO SAR. Compared to traditional anterograde GEO SAR, the proposed concept has the following advantages: (1) Shorter revisit time. The orbital period of traditional anterograde GEO and sub retrograde synchronous orbit SAR is nearly 24 hours. Due to the relatively fast satellite flight speed of sub retrograde synchronous orbit SAR, it brings shorter revisit time.(2) Better resolution. Traditional GEO SAR is greatly affected by the Earth's rotation, resulting in non orthogonal two-dimensional imaging resolution, thereby reducing the imaging resolution. However, the retrograde GEO SAR is observed in side looking at different positions throughout the orbit, so its two-dimensional resolution is orthogonal. (3) Simpler timing. The azimuth Doppler bandwidth of conventional GEO SAR is time-varying. When designing the system timing, it is necessary to consider the impact of changes in azimuth ambiguity caused by Doppler bandwidth variant. For retrograde synchronous orbit SAR, the satellite speed is constant, so its Doppler bandwidth is also constant. Therefore, the system timing design only needs fixed design.

The organizational structure of this article is as follows. The second section analyzes the orbital characteristics of sub retrograde GEO SAR which focuses on the satellite geometric relationship, satellite velocity, synthetic aperture time, Doppler frequency, Doppler modulation frequency, observation coverage and yaw angle. The third section is the design of radar parameters, including system sensitivity analysis, resolution analysis and timing analysis. Based on the definition of resolution, a high-precision azimuth resolution analysis method is proposed. In fourth section, the imaging characteristics of sub retrograde GEO SAR are studied. The Chirp Scaling algorithm is used for sub retrograde GEO SAR imaging processing. The influence of orbit perturbation error in sub retrograde GEO SAR is given for the first time. The fifth section gives two ways to solve the observation blind areas, one way is to change the orbit inclination, the another way is to use the bistatic mode.

II. Characteristic Analysis of Sub Retrograde GEO SAR

A. Analysis of satellite geometric relationship

The geometry of GEO SAR is shown in Fig. 1. O is the earth center and O_s is the satellite, Ω is the right ascension of the ascending node (RAAN), i is the orbit inclination and u is the argument of perigee. $OXYZ$ is the earth inertial coordinate system (ECI), $OX'Y'Z'$ is the satellite orbit coordinate system, $\mathbf{u}_r$, $\mathbf{u}_p$, $\mathbf{u}_t$ is unit vectors of X', Y', Z', respectively. $\mathbf{R}_s$ and $\mathbf{R}_t$ are the position vectors of the satellite and the target, respectively. $\dot{\mathbf{R}}_s$ and $\dot{\mathbf{R}}_t$ are the first-order time derivative.

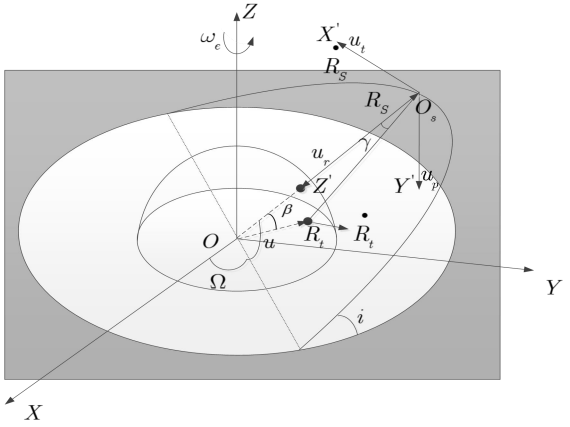

Fig. 1. Illustration of GEO SAR geometry.

The orbital parameters are shown in Table I. The orbit trajectory of sub retrograde GEO SAR in ECI coordinate system is shown in Fig. 2.

TABLE I
SIMULATION PARAMETERS

orbit height	35738 km
inclination	180°
eccentricity	0°
ascending node	110°
the perigee angle	0°
the true perigee angle	90°
the carrier frequency	1.25 GHz
the radar off-nadir angle	3°
the range beam width	0.4°
the azimuth beam width	0.4°

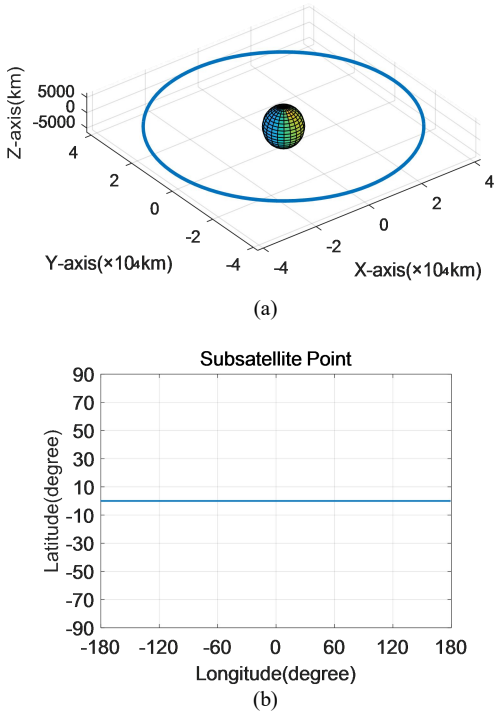

Fig. 2. Space trajectory under sub retrograde GEO:(a) ECI, (b) Sub-satellite point.

B. Satellite speed analysis

The beam foot-mark velocity vector $\mathbf{V}_{sg}$ can be expressed by

$$\mathbf{V}_{sg}=\frac{|\mathbf{R}_t|\cdot\cos\beta}{|\mathbf{R}_s|}\mathbf{V}_s-\mathbf{V}_t \tag{1}$$

where β is the angle between $\mathbf{R}_s$ and $\mathbf{R}_t$, $\mathbf{V}_s$ and $\mathbf{V}_t$ are the velocity vectors of the satellite and the target, respectively.

The velocity of the satellite relative to the earth $\mathbf{V}_{s\_eq}$ can be rewritten as

$$\mathbf{V}_{s\_eq}=\frac{|\mathbf{R}_s|}{|\mathbf{R}_t|\cdot\cos\beta}\mathbf{V}_{sg}=\mathbf{V}_s-\frac{|\mathbf{R}_s|}{|\mathbf{R}_t|\cdot\cos\beta}\mathbf{V}_t \tag{2}$$

It can be seen that the sub retrograde synchronous orbit SAR has little change about the track velocity and beam foot-mark velocity in the whole orbit, so the variation of velocity related parameters such as azimuth Doppler spatial variation and synthetic aperture time variation will be small, which is contribute to imaging processing.

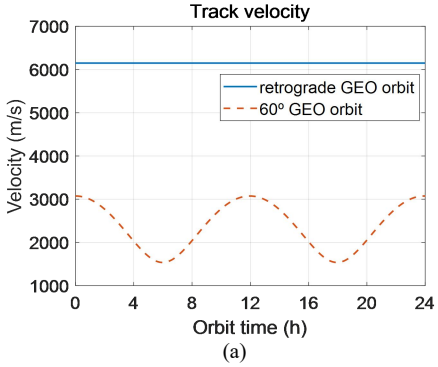

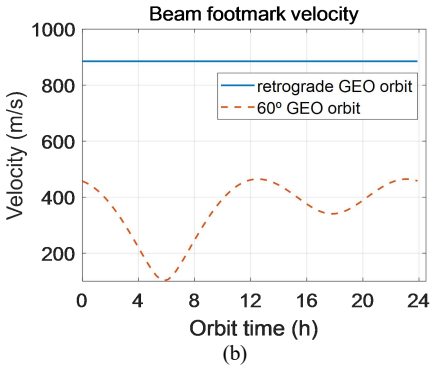

Fig. 3. Satellite speed:(a) Inertia velocity, (b) Beam foot-mark velocity.

The change of satellite velocity and beam foot-mark velocity in conventional GEO SAR reach 1600 m/s and 350 m/s respectively in the whole orbit. The change will affect the Doppler characteristics of imaging, including Doppler frequency, Doppler bandwidth and so on.

C. Synthetic aperture time

Synthetic aperture time is defined as the time span when the target is in the radar 3 dB beam. The traditional synthetic aperture time calculation formula of LEO SAR can be expressed as [48]

$$T_a=\frac{R_0\theta_{az}}{V_{sg}} \tag{3}$$

where R_0 the distance from the satellite to the pointing target of the beam center, θ_{az} is the beam width of azimuth, and V_{sg} is the ground footprint speed of the beam which is the absolute value of the beam ground speed vector $\mathbf{V}_{sg}$. The formula assumes that the synthetic aperture trajectory is a linear trajectory, and the velocity in the linear trajectory is a uniform linear motion, but the motion trajectory of GEO SAR is seriously curved and the velocity time-varying is strong. Therefore, the above synthetic aperture time calculation formula is no longer applicable to GEO SAR.

A new method for calculating synthetic aperture time is presented, that is, to judge whether the ground reference target is within the radar 3dB beam, and calculate the satellite's time in the beam point by point to accumulate. The following inequality can be used to infer whether the angle of view from the radar to the target is within the beam

$$\frac{4(\theta_r-\theta_{r0})^2}{\theta_{rg}^2}+\frac{4\theta_a^2}{\theta_{az}^2}\le 1 \tag{4}$$

where θ_r is the elevation angle and θ_a is the azimuth angle in antenna coordinate system, θ_{r0} is the radar off-nadir angle, θ_{rg} is half of the range beam width, θ_{az} is half of the azimuth beam width.

The geometry of variables in antenna coordinate system is shown in Fig. 4. Assuming the radar frequency band is the L-band and the radar off-nadir angle is 3°, the range and azimuth beam width is 0.4°.The synthetic aperture time with 5 m resolution is shown in Fig. 5.

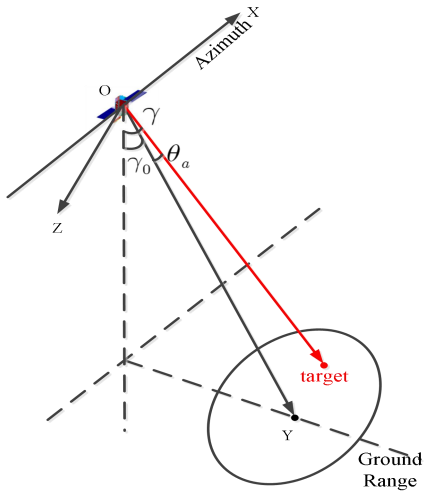

Fig. 4. The geometry of variables in synthetic aperture time calculation.

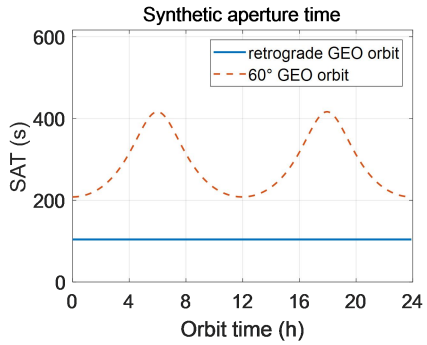

Fig. 5. Synthetic aperture time of 5 m resolution under sub retrograde GEO orbit and 60°-inclined GEO SAR.

The synthetic aperture time of conventional GEO SAR is different at different orbital positions. However, for the sub retrograde GEO, the synthetic aperture time of the whole orbit is a constant value because of the satellite's flight speed is uniform. Due to the high flight speed of the sub retrograde synchronous orbit SAR satellite, the synthetic aperture time required under the same resolution is less than that of the conventional GEO SAR.

D. Doppler characteristics

Doppler characteristic is the key factor of SAR satellite imaging. It is depended on satellite orbit, off-nadir angle, antenna pointing, earth rotation and so on.

The Doppler parameter calculation method based on the geometric relationship between satellite and ground is used to describe the instantaneous Doppler frequency, which can be expressed as

$$f_d = -\frac{2}{\lambda}\dot{R} = -\frac{2}{\lambda R}\left(\mathbf{R_s}-\mathbf{R_t}\right)\cdot\left(\dot{\mathbf{R}}_s-\dot{\mathbf{R}}_t\right) = -\frac{2}{\lambda R}\mathbf{R}\cdot\mathbf{V_{st}} \quad (5)$$

where the velocity vector of the satellite relative to the point target $\mathbf{V_{st}} = \dot{\mathbf{R}}_s - \dot{\mathbf{R}}_t$.

The Doppler frequency modulation can be obtained by deriving the Doppler frequency as

$$\gamma_a = \frac{\partial f_d}{\partial t} = -\frac{2}{\lambda}\ddot{R} = -\frac{2}{\lambda R}\left(\left|\mathbf{V_{st}}\right|^2 + \mathbf{R}\cdot\mathbf{A_{st}} - \frac{\left(\mathbf{V_{st}}\cdot\mathbf{R}\right)^2}{R^2}\right) \quad (6)$$

where the acceleration vector of the satellite relative to the point target $\mathbf{A_{st}} = \ddot{\mathbf{R}}_s - \ddot{\mathbf{R}}_t$. Assume that the radar works in C-band, the Doppler frequency and the Doppler modulation frequency of the sub retrograde GEO SAR and the conventional GEO SAR are shown in Fig. 6 and Fig. 7.

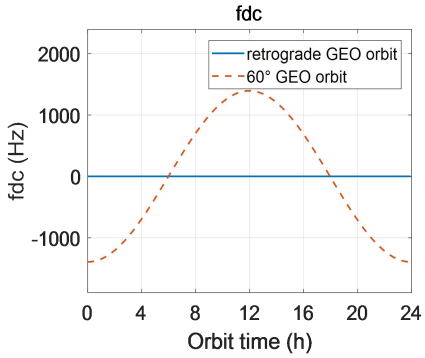

Fig. 6. Doppler center frequency under sub retrograde GEO orbit and 60°-inclined GEO SAR.

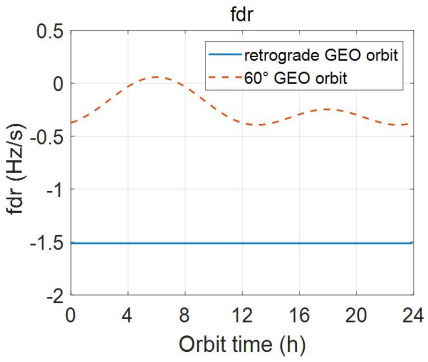

Fig. 7. Doppler frequency modulation under sub retrograde GEO orbit and 60°-inclined GEO SAR.

It can be seen that the Doppler frequency and Doppler frequency modulation rate of sub retrograde GEO satellite SAR change little in the whole orbit, and its azimuth resolution characteristics and imaging characteristics are relatively constant in the whole orbit.

E. Observation area

In order to get the observation area of the beam on the ground, we need to calculate the direction of the beam, and then get the footprint of the beam on the ground according to the direction of the beam. In the satellite body coordinate system, the beam direction can be determined by the angle of range γ and azimuth θ_a, which can be expressed by

$$\begin{aligned}\mathbf{Q} &= \sin\theta_a u_t + \cos\theta_a\left(\cos\gamma u_r + \sin\gamma u_p\right)\\ &= \sin\theta_a u_t + \cos\theta_a\sin\gamma u_p + \cos\theta_a\cos\gamma u_r\end{aligned} \quad (7)$$

where u_t', u_p', u_r' represents the unit vectors corresponding to the three axes in the satellite body coordinate system, $\gamma > 0$

means right-side looking, $\gamma < 0$ means left-side looking, $\theta_a > 0$ means forward looking, $\theta_a < 0$ means back looking.

After the direction of the beam is determined, according to the earth ellipsoid equation, we can get the footprint of the beam on the ground, so as to get the coverage of the beam on the ground. The detailed derivation process can be seen in reference [49].

Satellite tool kit (STK) is used to simulate the coverage observation area of LEO, conventional GEO and sub retrograde GEO respectively in Fig.8. The incidence angles of the three orbits are all 10° to 60°, the azimuth and range angle of sub retrograde GEO SAR is $\pm 3°$,while traditional GEO SAR is ±3°, LEO SAR is ±45°.

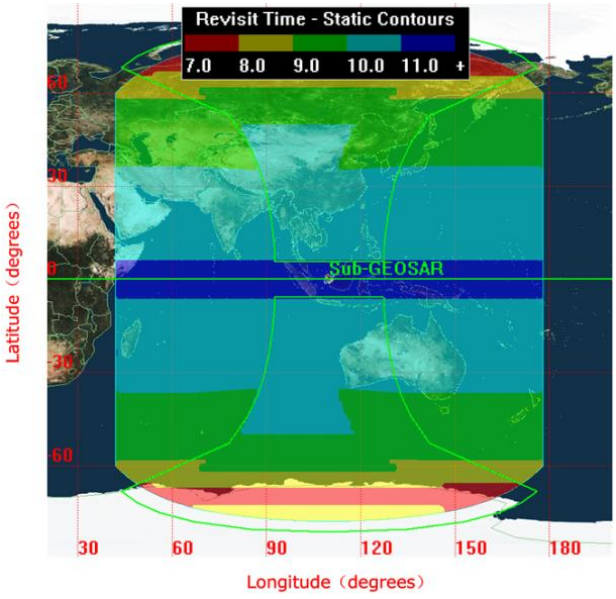

(a)

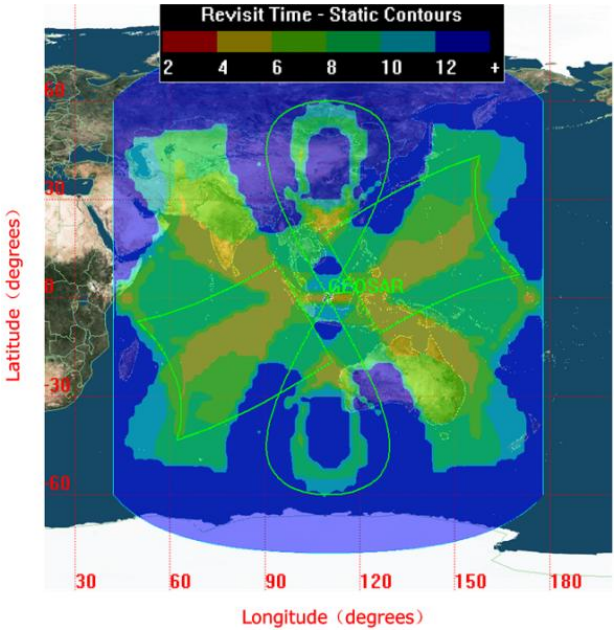

(b)

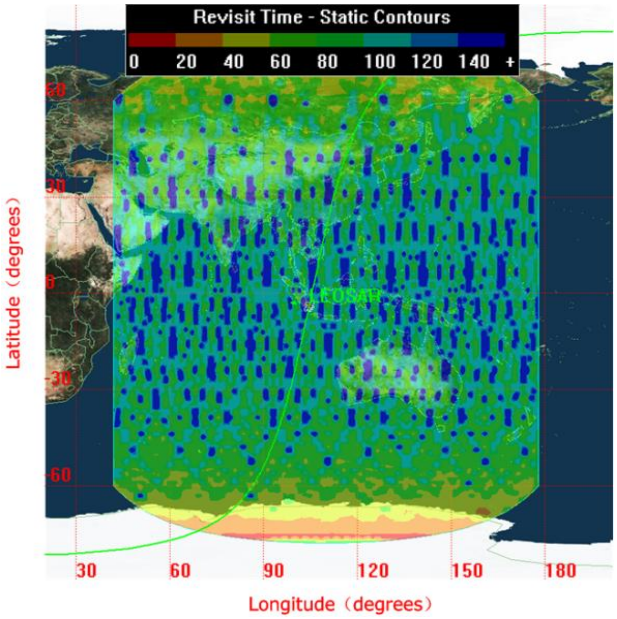

(c)

Fig. 8. Revisit time of a cycle:(a) sub retrograde GEO SAR, (b) GEO SAR with 60° inclination angle, (c) LEO SAR.

TABLE II
REVISIT AND ACCESS DURATION TIME

	Sub-GEO	GEO	LEO
Revisit time (h)	9.5-10	12-14	14-18
Access duration time (min)	90-100	540-600	3.5-4

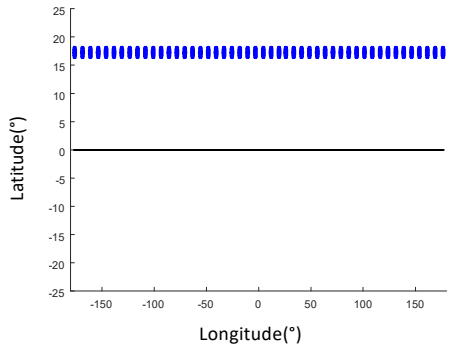

(a)

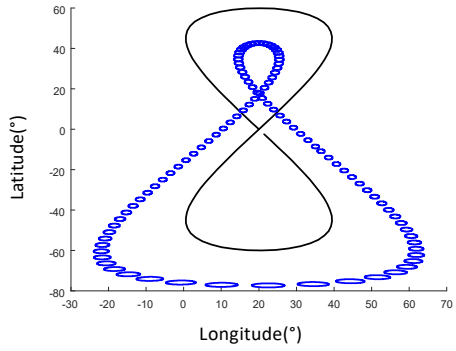

(b)

Fig. 9. Beam footprint area:(a) sub retrograde GEO, (b) 60°-inclined GEO SAR.

It can be seen that the observation performance of sub retrograde synchronous orbit SAR is much better than that of LEO SAR, conventional GEO SAR can only realize regional observation. Figure 9 shows that the beam footprints of conventional GEO SAR are mainly distributed in the North-South direction. However, for sub retrograde synchronous orbit SAR, its coverage area is global, not specific longitude and latitude, and its beam coverage mainly depends on the observation angle. For the Peking region observation performance shown in Table II, the revisit time of sub retrograde GEO SAR is better than that of GEO SAR and LEO SAR,but the sustainable time of sub retrograde GEO SAR is worse than GEO SAR and better than LEO SAR.

F. Yawing steering

The combination of the satellite's own speed and the earth's rotation speed will make the actual flight direction of the satellite deviate from the original trajectory, which leads to the so-called yaw angle.

The yaw angle can be expressed by

$$\begin{aligned}\mathbf{P} &= \dot{\mathbf{R}}_s - \omega_e \mathbf{k} \times \mathbf{R}_s \\ &= \left(\frac{h}{r} - r\omega_e \cos i\right)\mathbf{u}_t - r\omega_e \sin i \cos u \mathbf{u}_p - \frac{h}{p} e \sin f \mathbf{u}_r\end{aligned} \tag{8}$$

where r is the scalar of satellite orbit position, $\mu = 398600.4\ \mathrm{km}^3/\mathrm{s}^2$ is the gravitational constant of the earth, $\omega_e = 2\pi/T_s = 7.2921\times10^{-5}\ rad/s$ is the rotation speed of the earth, $\omega_s = \omega_e$ is the average angular velocity of satellite, $p = a\left(1-e^2\right)$, $h = \sqrt{\mu p}$. The yaw angles of conventional GEO SAR and the sub retrograde GEO SAR are shown in Fig.10. For conventional GEO SAR, due to the influence of earth rotation, there is a large yaw angle. After one-dimensional yaw traction processing, under the same resolution, the full orbit synthetic aperture time is less than that without yaw traction. When there is no yaw traction, the synthetic aperture time of the whole orbit is very long, especially at the apogee, which is due to the large squint observation geometry. It can be found from the analysis of references [49] that the one-dimensional yaw guidance shift can significantly improve the synthetic aperture time. For sub retrograde GEO SAR, the yaw angle can be found to be zero through simulation analysis. In this case, the imaging will not introduce squint angle, which greatly reduces the coupling between range and azimuth.

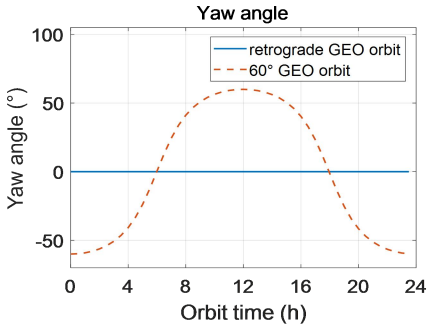

Fig.10. Yaw angle under sub retrograde GEO and 60°-inclined GEO.

III. System Parameter Design

A. Transmit power analysis

Due to the high orbit position and long operating range, in order to meet the signal-to-noise ratio requirements of the imaging, a large power aperture product is required, the noise equivalent sigma zero($NE\sigma^0$) is calculated by

$$NE\sigma^0 = \frac{(4\pi)^3 R_s^4 (kT_0) BFLL_{OA}^2 M}{P_t G_a^2 \lambda^2 G_{\mathrm{int}} G_{comp} \rho_{az} \rho_{gr}} \tag{9}$$

where R_s is the slant range from the radar to the target point, P_t is the total transmission power of the radar, L is the system link loss, G_a is the antenna gain, L_{OA} is the off-axis loss of the antenna, σ^0 is the radar back scattering coefficient, ρ_a is the azimuth resolution, ρ_r is the range resolution, F is the receiver noise factor, B is the signal bandwidth, λ is the wavelength, G_{comp} is the pulse compression ratio, G_{int} is the azimuth accumulation gain, $k = 1.380\times10^{-23}$ is the Boltzmann constant, M is the system margin.

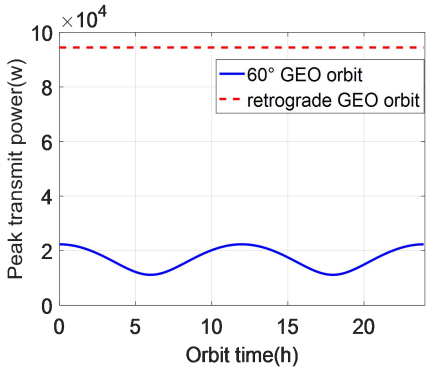

Fig. 11. Peak power of sub retrograde GEO and 60°-inclined GEO SAR.

The peak transmission power required for different orbital positions of the conventional GEO SAR and the sub retrograde GEO SAR are shown in the Fig. 11. The simulation parameters are selected as follows: the antenna aperture is 40 m, the receiver noise factor is 2 dB, and the system loss is 3 dB, $NE\sigma^0$ is -20 dB, the peak transmit power is 100 kw, the center frequency point is 1.25 GHz, the off-axis loss of the antenna is 3 dB, the slant range from the radar to the target point is 35738 km, the antenna gain is approximately 52 dB, the range resolution is 5 m. Under the same resolution, the transmission power required for different positions of the whole orbit of conventional GEO SAR is different, while the transmission power required of the whole orbit in sub retrograde GEO SAR is the same.

B. Azimuth resolution

The azimuth resolution of airborne SAR and traditional LEO SAR is approximately half of the radar antenna length. Due to the high orbital altitude and the great influence of earth rotation on effective radar velocity and Doppler parameters, GEO SAR has a long synthetic aperture time and a curved trajectory that can't be ignored, so the traditional azimuth resolution calculation method based on uniform linear motion

trajectory are no longer applicable.

According to the Doppler characteristic at the different times and the satellite speed analyzed previously, we can get the calculation formula [50] of the GEO SAR azimuth resolution as

$$\rho_{AZ} = \frac{\sqrt{\mathbf{V}_{sg} \cdot \mathbf{V}_{s\_eq}}}{B_a} \tag{10}$$

where B_a is the Doppler bandwidth.

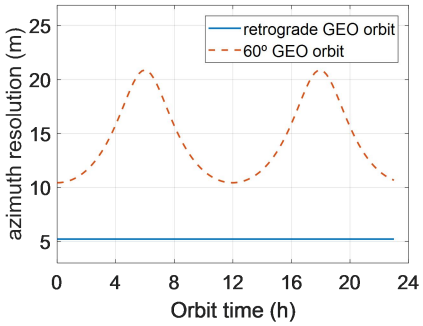

Fig. 12. Azimuth resolution with synthetic aperture time of 100 s under sub retrograde GEO and 60°-inclined GEO SAR.

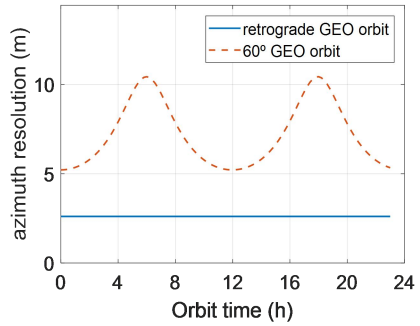

Fig. 13. Azimuth resolution with synthetic aperture time of 200 s under sub retrograde GEO and 60°-inclined GEO SAR.

Fig.12 and Fig.13 shows that the azimuth resolution of the conventional GEO SAR and the sub retrograde GEO SAR when the synthetic aperture time is 100s and 200s, respectively. It can be seen that the resolution of sub retrograde GEO SAR is constant in the whole orbit, but the azimuth resolution is very different when the satellite runs in the conventional GEO SAR.

C. Timing design

The pulse repetition frequency (PRF) of space-borne synthetic aperture radar needs to be strictly designed according to the observation angle. When PRF is selected, the factors such as azimuth ambiguity, range ambiguity and sub-satellite point echo need to be considered. For sub retrograde GEO SAR, the squint angle is 0°. At this time, the radar timing design does not need to consider the case of range migration caused by squint angle as described in PRF, which greatly simplifies the timing design of the system.

PRF must satisfy the following equation [51]

$$\frac{m}{\frac{2R_n}{c} - \frac{2H_L}{c} - T_{w-nadir}} < PRF < \frac{m+1}{\frac{2R_f}{c} - \frac{2H_L}{c} + T_p} \tag{11}$$

where R_n is the proximal slant range and R_f is the distal slant range in swath, H_L is the distance between satellite and nadir point, T_p is pulse width, $T_{w-nadir}$ is duration time of nadir echo and m is an integer.

To avoid emitting block, PRF must satisfy the following equation

$$\frac{n}{\frac{2R_n}{c} - T_p - T_g} < PRF < \frac{n+1}{\frac{2R_f}{c} + T_p + T_g} \tag{12}$$

where T_g is the guard time, n is the number of emitted pluses between transmission and reception and which can also be approximated by $n=\text{int}\left(2R_n/c \cdot \text{PRF}\right)=\text{int}\left(2R_f/c \cdot \text{PRF}\right)$, where int() indicates the floored integer.

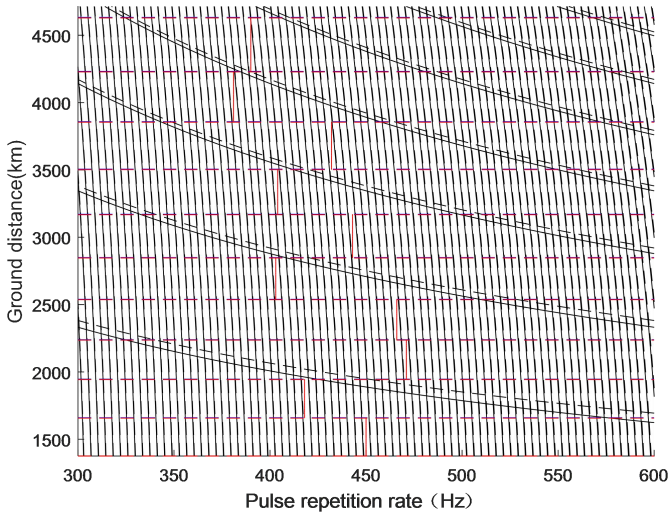

Fig. 14. Zebra map of sub retrograde GEO

According to the timing design results, as shown in Fig. 14, PRF selection of sub retrograde GEO SAR is 400 ~ 500 Hz, which can meet the azimuth ambiguity and range ambiguity required for imaging, as shown in Fig. 15.

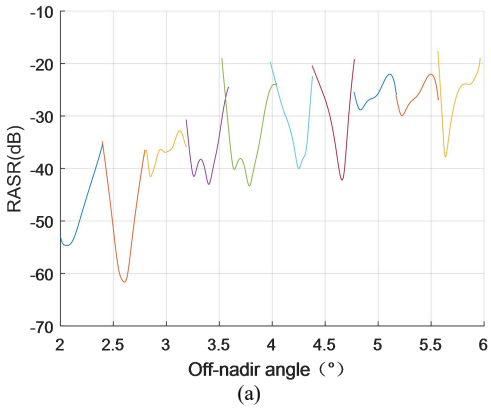

(a)

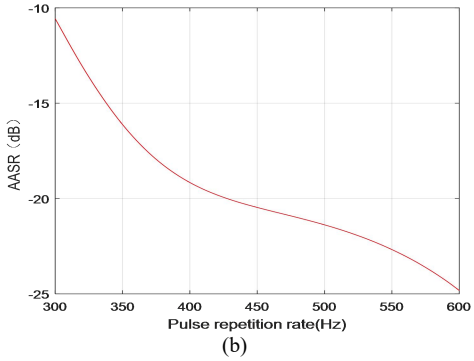

Fig. 15. Ambiguity analysis of the sub retrograde GEO SAR:(a) RASR, (b) AASR.

Due to its Doppler characteristics changing with orbital position in conventional GEO SAR, timing design needs to be changed at different orbital positions. The figure 16 shows the different AASR values obtained under the same PRF at different orbital positions, indicating that the same PRF at different orbital positions brings different AASR values. Therefore, we can get that the timing of the traditional anterograde GEO SAR is orbital variant, but invariant for the sub retrograde GEO SAR.

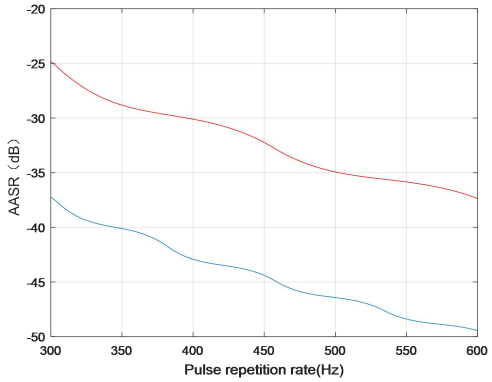

Fig. 16 AASR of the 60°-inclined GEO SAR.

IV. Study on Imaging Characteristics

A. Slant range model

For conventional GEO SAR, the slant range model is usually extended to fourth order [52], as shown below

$$\mathbf{R}(t_a)=\mathbf{R}_{st}+\mathbf{V}_{st}t_a+\frac{1}{2}\mathbf{A}_{st}t_a^2+\frac{1}{6}\mathbf{B}_{st}t_a^3+\frac{1}{24}\mathbf{C}_{st}t_a^4 \quad (13)$$

where $\mathbf{R}_{st}, \mathbf{V}_{st}, \mathbf{A}_{st}, \mathbf{B}_{st}, \mathbf{C}_{st}$ are the first, second, third and fourth derivatives of the vector of satellite position and target respectively, t_a is the azimuth slow time.

When the orbit inclination is 180°, the slant range history error results obtained by different order models are respectively shown in Fig. 17. It can be seen that when the slant range order is taken to the third order, the slant range error is less than 0.03 m, which can not meet the requirements of less than 1/32 wavelength accuracy in the imaging processing.Thus, the four-order range model is required for both the traditional and sub retrograde GEO SAR .

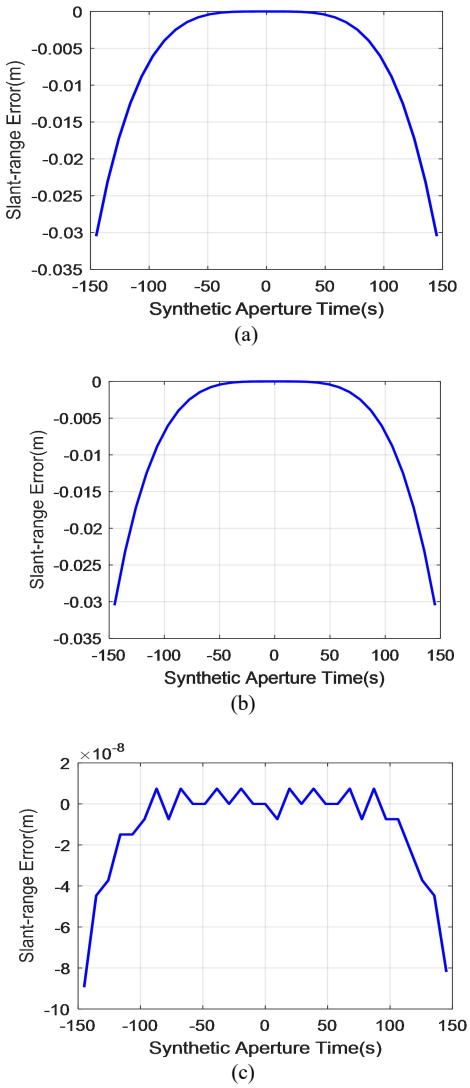

Fig. 17. Different order slant-rang error of sub retrograde GEO:(a) second order, (b) third order, (c) fourth order.

B. Range space-variant

Range space-variant refers to the characteristic that the signal model changes with the distance and position of the point target. Under the traditional low orbit SAR strip mode, the imaging swath is only tens of kilometers, and with the rise of satellite orbit, the imaging swath also increases. Under GEO SAR strip mode, the swath can reach 300km, and the range space-variant increases significantly. The slant distance difference of range cell migration along the range direction can be expressed as

$$\delta\mathbf{R}(t_a;R_n)=\mathbf{R}(t_a;R_n)\text{-}\mathbf{R}(t_a;R_c) \quad (14)$$

where R_c is the shortest slant range from radar to the center point, R_n is the shortest slant range from radar to the reference point.

We assume that there are five target points in the imaging scene as shown in Fig. 18. The four points are -75 km, 75 km, -150 km and 150 km away from the center point along the distance direction. The incident angle of the scene center point is 40°, and the synthetic aperture time is 300 s.

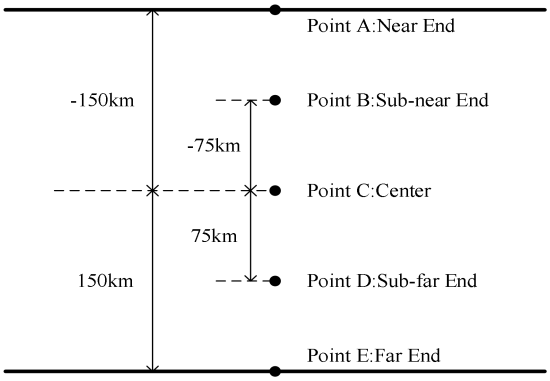

Fig. 18. Target positions along the distance direction in the scene

The one-way slant distance differences between the scene center point and the four point targets are given respectively shown as in Fig.19 and Fig.20.

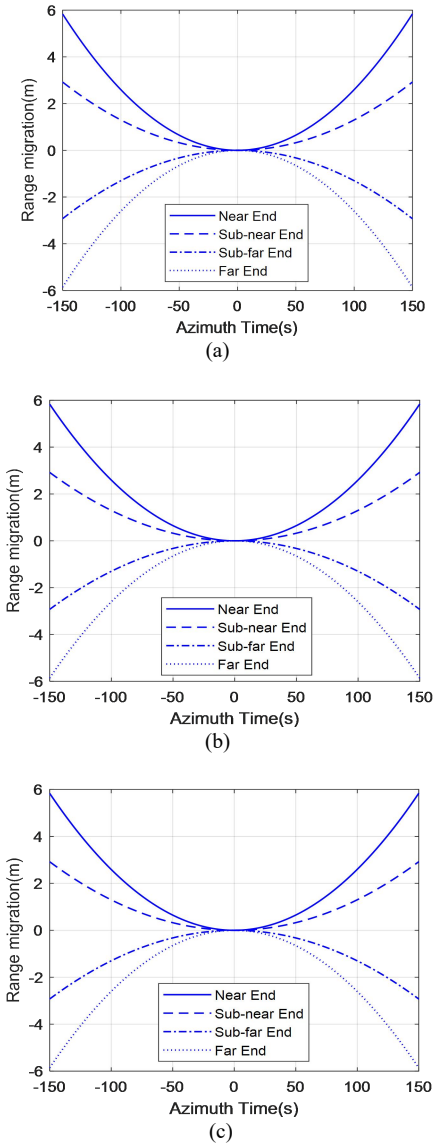

Fig. 19. Range space-variant of sub retrograde GEO:(a) at the perigee, (b) at 3 hour after perigee, (c) at 6 hour after perigee.

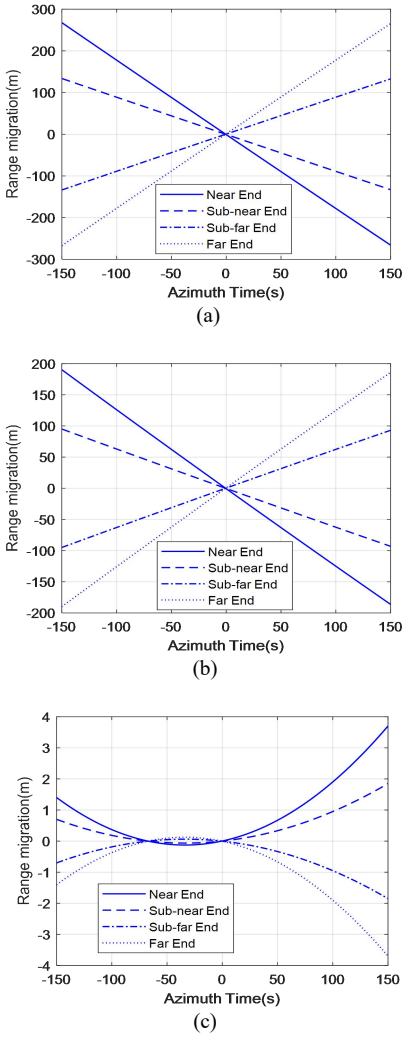

Fig. 20. Range space-variant of 60°-inclined GEO SAR:(a) at the perigee, (b) at 3 hour after perigee, (c) at 6 hour after perigee.

From the range space-variant at the perigee 0, 3 and 6 hour, it can be seen that the range space-variant at different orbit times is the same and only a few meters. But for conventional GEO SAR, its range space-variant can reach tens of meters or even hundreds of meters, spanning multiple range units.

C. Azimuth space-variant

The classical frequency domain imaging processing algorithms are generally based on meeting the azimuth time invariance, so as to realize batch compression of point target echoes with the same slant range in the azimuth frequency domain and improve the imaging processing efficiency. However, the synthetic aperture time of traditional GEO SAR is about hundreds of seconds. There is serious azimuth space-variant in the azimuth direction.

The distance difference of range cell migration caused by the azimuth space-variant can be expressed as

$$\Delta\mathbf{R}(t_m;R_c)=\mathbf{R}(t_m;R_c)\text{-}\mathbf{R}(t_c;R_c) \qquad (15)$$

where t_c represents the beam center crossing time of center point, t_m represents the beam center crossing time of reference point.

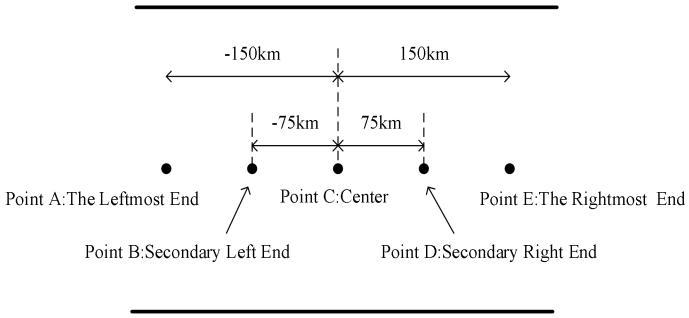

Fig. 21. Target positions along the distance direction in the scene.

It is assumed that the orbital inclination is 60°, and the synthetic aperture time duration is 300 s. It can be seen that the one-way slant range errors of different point targets along the azimuth direction are far greater than the error tolerance, and the azimuth space-variant is strong, which will greatly reduce the processing and calculation efficiency of frequency domain algorithm, as shown in Fig. 22.

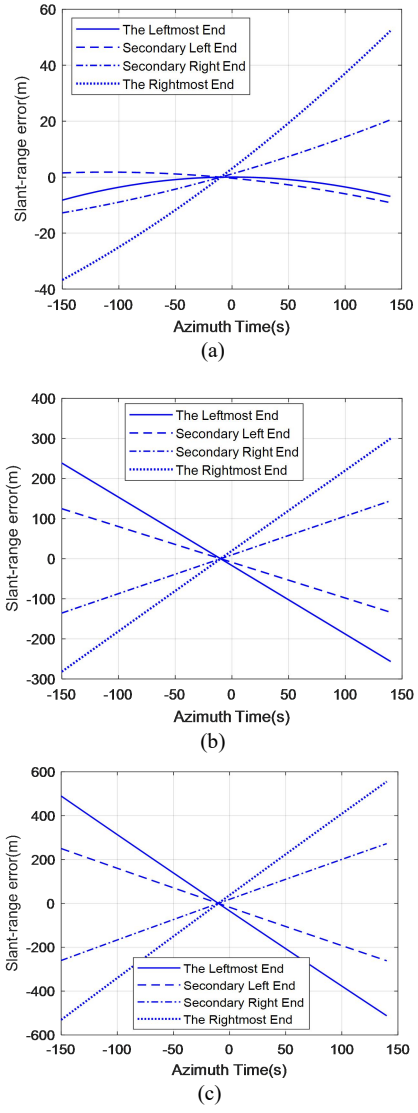

Fig. 22. Azimuth space-variant of 60°-inclined GEO SAR: (a) at the perigee, (b) at1 hour after perigee, (c) at 2 hour after perigee.

However, for sub retrograde GEO SAR, the azimuth space-variant is greatly reduced. The following Fig.23 gives the azimuth space-variant of four point targets which are 75 km and 150 km away from the reference point of the scene center respectively, and the synthetic aperture time is 300 s.The azimuth space-variant of sub retrograde GEO SAR at different times is far less than the error tolerance, it meets the azimuth time invariance.

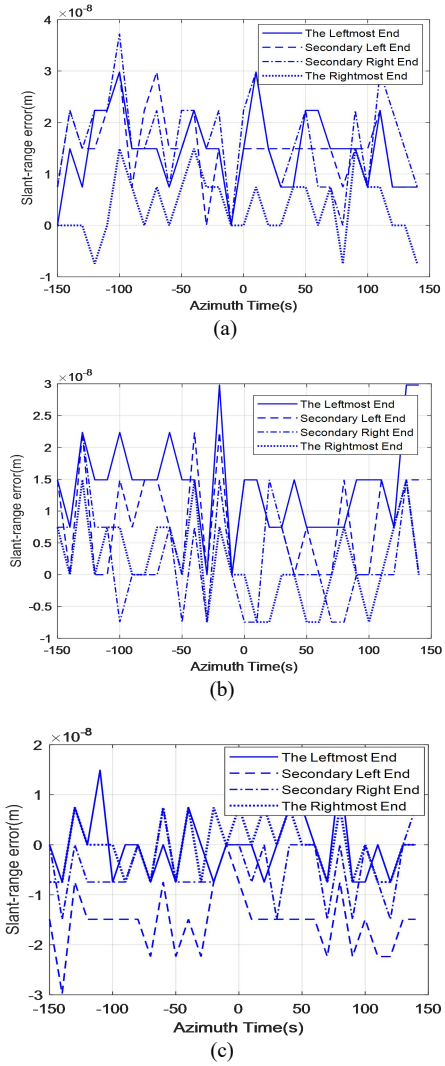

Fig.23. Azimuth space-variant of sub retrograde GEO:(a) at the perigee, (b) at1 hour after perigee, (c) at 2 hour after perigee.

D. Frequency imaging algorithm

For conventional GEO SAR, due to the long synthetic aperture time, squint angle caused by the earth's rotation, curved flight trajectory and other reasons, its slant range is expressed by fourth-order expression, and the coupling between azimuth and range direction is serious, and the azimuth space-variant is strong. The literature [53] puts forward the influence of traditional straight line model and an improved SPECAN algorithm based on the accurate range model, Literature [54] established the range model by using fourth-order approximation, and an improved imaging algorithm with sub-aperture processing method is proposed.

We use an improved CS algorithm [55] for the sub retrograde GEO SAR imaging, where the slant range model is expanded to fourth order.The following figure simulates the imaging of point targets of the sub retrograde GEO SAR at 0 hour after perigee with which the orbit inclination is 180°.Due to the velocity and Doppler frequency of the proposed GEO SAR is orbital invariant, one orbital position is enough to verify that the CS is effective. The synthetic aperture time is 300 s, the carrier frequency of the transmitted signal is 1.25 GHz, the time width is 1 us, and the bandwidth is 250 MHz. The results are given as follows. It can be seen that the imaging results of improved CS algorithm based on fourth-order range model can meet the imaging requirements.

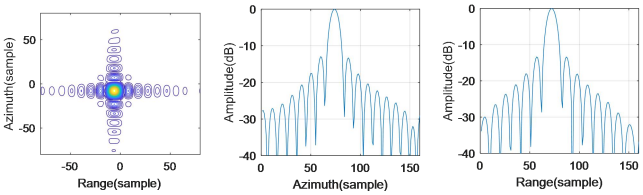

(a) (b) (c)

Fig. 24. CS algorithm imaging results of sub retrograde GEO at 0 hour after the perigee:(a) 2-D contour, (b) Range profile, (c) Azimuth profile.

TABLE III
IMAGING RESULT IN DIFFERENT ORBIT POSITION

Point target	Range			Azimuth		
	RE (m)	PSLR (dB)	ISLR (dB)	RE (m)	PSLR (dB)	ISLR (dB)
0h	1.00	-13.12	-9.65	1.84	-13.12	-10.65

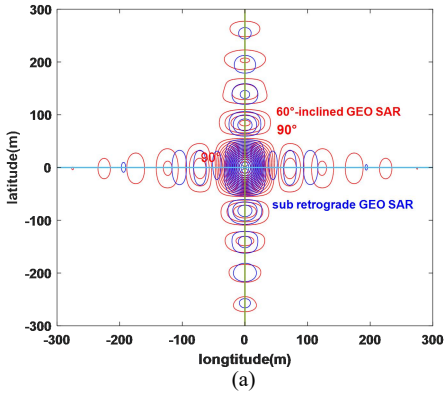

(a)

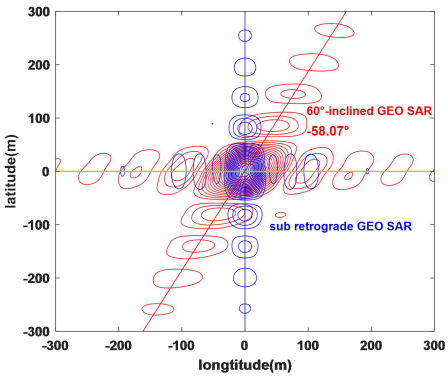

(b)

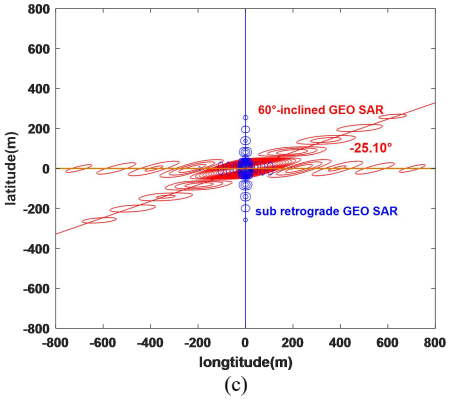

(c)

Fig. 25. Imaging results at different orbital positions:(a) at 0 hour after the perigee, (b) at 1 hour after the perigee, (c) at 3 hour after the perigee.

In order to compare the imaging differences between conventional GEO SAR and sub retrograde GEO SAR, imaging results at different orbital positions are presented. It can be seen that for conventional GEO SAR, due to the influence of the Earth's rotation,the azimuth and range angle is orthogonal at 0 hour past perigee. At 1 hour past perigee moment, the angle between the azimuth and range is 58.07°, indicating non orthogonality. At 3 hour past perigee moment, the angle between its azimuth and distance is 25.10°, showing its non orthogonality. The non orthogonal state of azimuth and distance can lead to a deterioration of resolution.On the other hand, for sub retrograde synchronous orbit SAR, the azimuth and range directions at different orbital positions are always orthogonal. From the Fig.25 , it can also be seen that within the same synthetic aperture time, the sub retrograde GEO SAR will achieve better azimuth resolution than traditional GEO SAR, which is due to the relatively fast operation speed of retrograde synchronous orbit satellites, resulting in a shorter acquisition time for the same resolution.

E. Influence of orbit perturbation error

The geometric relationship between accurate orbit and orbit with error is shown in Fig. 26.

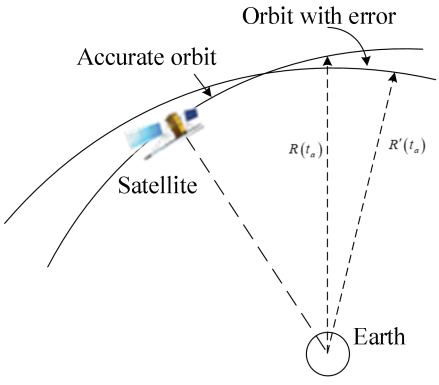

Fig. 26 Illustration of accurate orbit and orbit with error geometric.

When there is an error in the satellite position, the slant distance from the satellite to the point target will introduce an error term. The orbit error of GEO SAR can be approximately

regarded as the curve of N sine transforms, and the slant error term introduced by satellite orbit determination error can be expressed as

$$R_{error}\left(t_a\right)=A_a\sin\left(N\left(t_a+x_0\right)/T_s\right)+A_b \qquad (16)$$

where t_a is the azimuth time, x_0 is a random value which determines the variation trend of the error, T_s is the GEO SAR operation period, A_a is the amplitude of the relative error term, and A_b is the absolute error term.

In this case, the slant range error from radar to target point can be expressed

$$R'\left(t_a\right)=R\left(t_a\right)+R_{error}\left(t_a\right) \qquad (17)$$

where $R\left(t_a\right)$ is the scalar of slant distance from satellite to target point.

We assume that the amplitude of the relative error term A_a is 2 m, N is 12π and the absolute error A_b is 0.5 m, the synthetic aperture time is 300 s.

The previously proposed algorithm is used to carry out sub retrograde GEO SAR imaging simulation. Due to the velocity and Doppler frequency of the proposed GEO SAR is orbital invariant, one orbital position is enough to verify that the influence of orbit perturbation error is effective. The results are shown in the following.

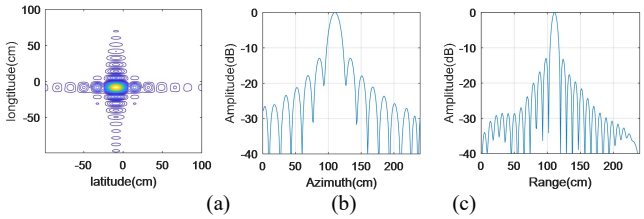

Fig.27. Imaging results of sub retrograde GEO at the perigee with orbit determination error:(a) 2-D contour, (b) Range profile, (c) Azimuth profile.

Compared with the imaging quality without orbital error and with orbital error, we can see from Table III and Table IV that the PLSR in the azimuth direction has deteriorated. With orbital error, the PSLR deteriorated 0.19 dB at the perigee.

Similarly, in order to compare the impact of orbital position error on conventional GEO SAR, we use the same parameters for imaging simulation. The results are shown in Fig. 28-30. It can be seen that the sub retrograde GEO SAR is less affected by the orbital position error, especially in PLSR. This is because of sub retrograde GEO SAR working in side-looking mode. But for the conventional GEO SAR, except at orbital time 0 hour, other positions are squint observation, which is greatly affected by orbital position error.

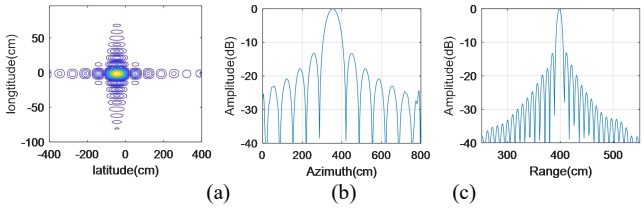

(b)

Fig. 28. Imaging results of 60°-inclined GEO SAR at the perigee with orbit determination error:(a) 2-D contour, (b) Range profile, (c) Azimuth profile.

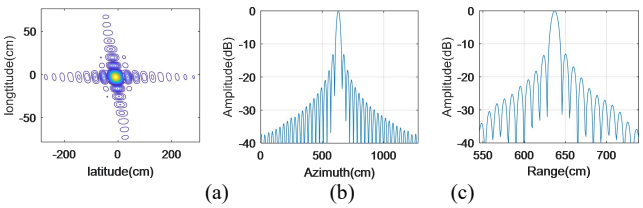

Fig.29. Imaging results of 60° -inclined GEO SAR at 1 hour after perigee with orbit determination error:(a) 2-D contour, (b) Range profile, (c) Azimuth profile.

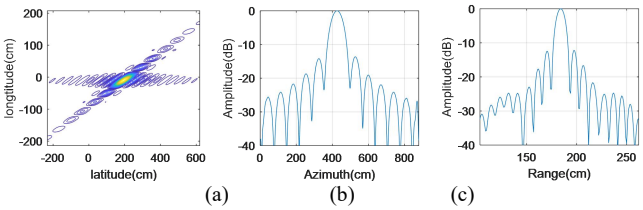

Fig. 30. Imaging results of 60°-inclined GEO SAR at 3 hour after perigee with orbit determination error:(a) 2-D contour, (b) Range profile, (c) Azimuth profile.

TABLE IV
IMAGING RESULT IN DIFFERENT ORBIT POSITION

Orbit	Point target	Range			Azimuth		
		RE (m)	PSLR (dB)	ISLR (dB)	RE (m)	PSLR (dB)	ISLR (dB)
sub retrograde	0h	1.00	-12.99	-9.83	1.88	-12.93	-10.13
60°-inclined	0h	1.00	-13.11	-9.68	7.37	-12.68	-10.17
	1h	1.25	-13.00	-9.92	10.13	-12.98	-9.94
	3h	2.76	-12.36	-9.68	23.75	-12.78	-9.56

V. SOLUTION OF OBSERVATION BLIND AREA

For sub retrograde GEO SAR, because its orbit is over the equator and its normal working mode is side looking, it is easy to lead to the existence of observation blind areas near the equator. There are two ways to solve this problem. One is to change the orbit inclination, for example, the orbit inclination of sub retrograde GEO SAR is not 180°. As shown in Fig. 31.

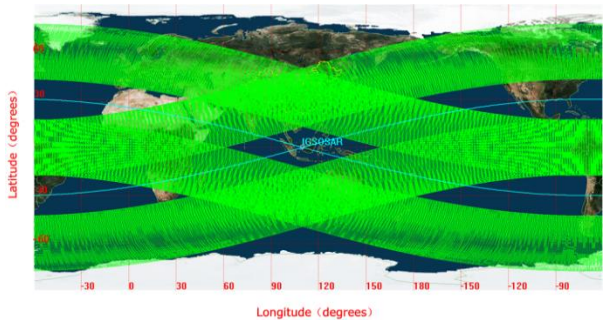

Fig. 31. Observation areas of the orbit inclination is not 180°.

After adjusting the orbit inclination, the area near the equator is covered by multiple satellite observations, so there is no observation blind area. However, the cost is that it is greatly affected by the earth's rotation. In addition, it will

cause the synthetic aperture time to become longer under the same resolution.

The synthetic aperture time required is shown as in Fig.32. The azimuth resolution is 5 meters when the inclination angle of the orbit is 150 °.

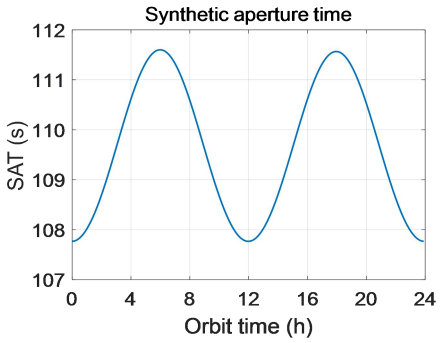

Fig. 32. Synthetic aperture time of 5 m resolution at 150°-inclined GEO SAR.

It can be seen that the synthetic aperture time required reaches 150s, which is greater than the synthetic aperture time required under the same resolution of 180° orbit inclination. This is mainly because the speed of the satellite relative to the ground decreases from 100 m/s to 50 m/s when the orbit inclination is 150°.

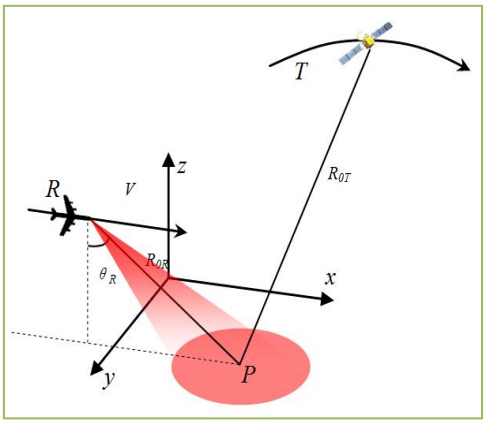

Fig. 33. Bistatic mode with GEO SAR and aircraft.

Another way is to use the bistatic mode to solve the problem. sub retrograde GEO SAR can be used as the irradiation source, and aircraft or LEO satellite can be used as the receiving platform. As shown in Fig. 33.

According to literature [56], in this mode, the resolution of bistatic underground imaging is

$$\rho_a = \frac{0.886\lambda}{\int_{t_0-T_a/2}^{t_0+T_a/2} \left\| H^{\perp}(\omega_{TA}(\mathrm{t}) + \omega_{RA}(\mathrm{t})) \right\| dt} \tag{18}$$

where λ is the signal wavelength, T_a is the synthetic aperture time. $\omega_{TA}(t)$ and $\omega_{RA}(t)$ are the angular velocities of the transmitter and the receiver, respectively, which are given by

$$\omega_{TA}(\mathrm{t}) = \frac{\left[\mathbf{I} - u_{TA}^{\mathrm{T}}(\mathrm{t}) u_{TA}(\mathrm{t})\right] V_T^{\mathbf{T}}}{\left\| P_A - R_T(\mathrm{t}) \right\|} \tag{19}$$

$$\omega_{RA}(\mathrm{t}) = \frac{\left[\mathbf{I} - u_{RA}^{T}(\mathrm{t}) u_{RA}(\mathrm{t})\right] V_R^{\mathbf{T}}}{\left\| P_A - R_R(\mathrm{t}) \right\|} \tag{20}$$

where $\mathbf{I}$ is the 3×3 identity matrix. P_A are the position of a point target, $R_T(\mathrm{t})$ and $V_T(\mathrm{t})$ are the position vector of GEO satellite, $R_R(\mathrm{t})$ and $V_R(\mathrm{t})$ are the position vector of the receiver.

With the special configuration of bistatic, the satellite nadir point of sub retrograde GEO SAR also has imaging ability. Assuming that the parameters of the receiving platform are the speed of 100 m/s, the height of the receiving platform is 50 km, the receiving antenna is 0.2 m and the receiving reflection angle is 55°, the range resolution and azimuth resolution can be obtained as shown in Fig. 34 and Fig. 35, respectively.

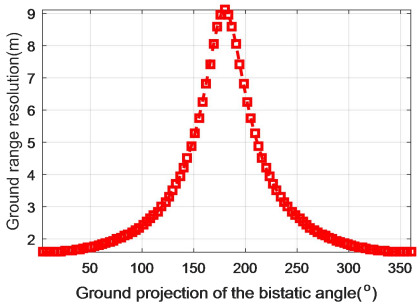

Fig. 34. Ground range resolution of the bistatic mode.

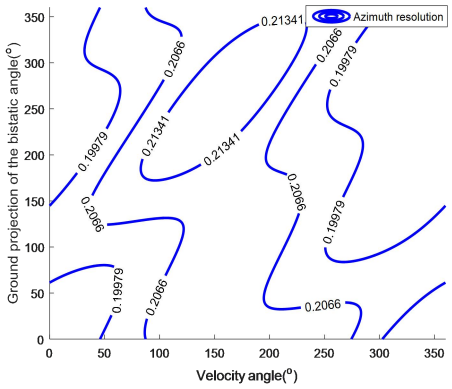

Fig. 35. Azimuth resolution of the bistatic mode.

VI. Conclusions

This paper presents a new concept of sub retrograde GEO SAR, and analyzes its orbit characteristics, focusing on the satellite geometric relationship, satellite velocity, synthetic aperture time, Doppler frequency, Doppler modulation frequency, observation coverage, yaw angle and so on. In the aspect of system design, the radar parameters are designed, including system sensitivity analysis, resolution analysis and timing analysis. The imaging characteristics of sub retrograde GEO SAR are studied, including range model, range and azimuth space-variant, imaging algorithm and so on. Finally, for this problem of observation blind area near the equator of sub retrograde GEO SAR, the way of changing orbit inclination and bistatic imaging is proposed. We find that the sub retrograde GEO SAR satellite has the advantages of uniform motion speed in the whole orbit, less influence by the earth's rotation, simple timing, shorter revisit time, better

resolution and small space-variant in azimuth and range. It can be used in disaster detection, topographic mapping, forest biomass, soil moisture, marine environment, marine target detection and other fields. For example, we can use the advantage of the short revisit time of the sub retrograde GEO SAR to monitor disasters, and we can also use its large coverage to achieve target detection at sea. The global three-dimensional topographic mapping can be realized by multiple repeated observations of sub retrograde SAR in different orbits.

Compared to conventional GEO SAR, sub retrograde orbit GEO SAR has some application advantages, but its cost is the need for larger transmission power and large aperture antennas. In order to realize the sub retrograde GEO SAR project, it is necessary to solve the problems of large aperture antenna and high-power transmission. At present, there are two methods. One is to build a large antenna, which is retracted during transmission and deployed on orbit. The other is to realize large aperture antenna by combining many small aperture antennas through distributed antenna, but this method needs to overcome the problem of coherent synthesis of signals. Besides, due to global observations, the sustainable observation time of sub retrograde orbit SAR for a certain region will be shorter than that of conventional GEO SAR when the orbital cycle time is fixed.

In addition, for sub retrograde GEO SAR, its application in interferometry and moving target detection also needs further research.

REFERENCES

[1]K. Tomiyasu, "Synthetic Aperture Radar in Geosynchronous Orbit ," in *Proc. Antennas Propag. Soc. Int. Symp*., vol. 16, pp. 42-45, May. 1978.

[2]K. Tomiyasu and L. J. Pacelli, "Synthetic aperture radar imaging from an inclined geosynchronous orbit," *IEEE Trans. Geosic. Remote Sens*., vol. GRS-21, no. 3, pp. 324-329, Jul. 1983.

[3]L. M. Murphy, "Synthetic Aperture Radar Imaging from Geosynchronous Orbit-Concept Feasibility and Applications," in *Int. Astronaut. Feder*., 1987, vol. 10, pp. 10-17.

[4]S. Madsen, W. Edelstein, L. Didomenico and J. LaBrecque, "A geosynchronous synthetic aperture radar; for tectonic mapping, disaster management and measurements of vegetation and soil moisture," in *Proc. IEEE IGARSS.,* 2001, vol. 1, pp. 447-449.

[5]S. Madsen, C. Chen and W. Edelstein, "Radar options for global earhquake monitoring," in *IEEE IGARSS*., vol. 3, 2022, pp. 1483-1485.

[6]W. Edelsteion, S. Madesen, A. Moussessian and C. Chen, "Concepts and technologies for synthetic aperture radar from MEO and geosynchronous orbit," in *Proc. SPIE*, Bellingham, USA, 2005, vol. 5659, pp. 195–203

[7]K. Gerhard, F. Hauke, R. C. Marc, H. David and M. Alberto, "System concepts for bi-and multi-static SAR missions," in *IRS, German Institute of Navigation*, 2003, pp: 331–339.

[8]Spaceborne earth surveillance radar systems [Online]. Available: http://www.vega.su/publ/Verba English Summary 1-13.pdf

[9]S. Hobbs, "GeoSAR Summary of the Group Design Project," MSc in *Astronaut. Spac. Eng*., no. 6, pp. 1-20, 2005.

[10]D. Bruno, S. E. Hobbs and G. Ottavianelli, "Geosynchronous synthetic aperture radar: Concept design, propertics and possible applications," *Acta Astonautica*, vol. 59, no. 1-5, pp. 149-156, 2006.

[11]J. Ruiz Rodon, A. Broquestas, E. Makhoul, A. Monti Guarnieri and F. Rocca, "Results on spatio-temporal atmospheric phase screeen retrieval from long-term GEOSAR acquisition," in *Proc. IEEE IGARSS*, Munich, Germany, Jul. 22-27, 2012, pp. 3289-3292.

[12]J. Ruiz Rodon, A. Broquetas, A. Monti Guarnieri and F. Rocca, "Geosynchronous SAR Focus-ing With Atmospheric Phase Screen Retrieval and Compensation," *IEEE Trans. Geosci. Remote Sens*., vol. 51, no. 8, pp. 4397-4404, Aug. 2013.

[13]J. Ruiz Rodon, A. Broquetas, A. Monti Guarnieri and F. Rocca, "A ku-band geosynchronous synthetic aperture radar mission analysis with medium transmitted power and medium-sized antenna," in *Proc. IEEEE IGARSS*, Vancouver, BC, Canada, Jul. 24-29, 2011, pp. 2456-2459, no. WE2.TO4.3.

[14]A. Recchia, A. M. Guarnieri, A. Broquetas and J. Ruiz-Rodon, "Assesment of atmospheric phase screen impact on Geosynchronous SAR," in *Proc. IEEEE IGARSS*, 2014, pp. 2253-2256.

[15]A. Recchia, A. M. Guarnieri, M. Belotti, D. Giudici, A. Leanza. "Demonstrative geosyn-chronous SAR products affected by clutter and APS decorrelation," in *Proc. IEEE IGARSS*, 2015, pp. 1265-1268.

[16]A. Recchia, A. M. Guarnieri, A. Broquetas, A. Leanza. "Impact of Scene Decorrelation on Geosynchronous SAR Data Focusing," *IEEE Trans. Geosci. Remote Sens.*, vol. 54, no. 3, pp. 1635-646, Mar. 2016.

[17]G. Wadge, A. Monti Guarnieri, S. E. Hobbs and D. Schultz, "Potential atmospheric and terrestrial applications of a geosynchronous RADAR," in *Proc. IGARSS*, Jul. 13-18, 2014, pp. 946-949.

[18]A. Monti Guarnieri, F. Rocca and A. B. Ibars, "Impact of atmospheric water vapor on the design of a Ku band geosynchronous SAR system," in *Proc. IEEE IGARSS*, Cape Town, Republic of South Africa, Jul. 12-17, 2009, vol. 2, pp. II-945-II-948.

[19]A. Monti Guarnieri *et al.*, "Design of a geosynchronous SAR system for water-vapour maps and deformation estimation," in *Fringe*, Paris, France, 2011, ESA SP-697.

[20]A. Monti Guarnieri *et al.*, "Wide coverage, fine resolution, geosynchronous SAR for atmospheric and terrain observation," presented at the *Living Planet Symp.*, paper no. ESA SP-722, 2013.

[21]L. Iannini and A. Monti Guarnieri, "Atmosphere phase screen in ground-based radar: Statistics and compensation," *IEEE Geosci. Remote Sens. Lett*., vol. 8, no. 3, pp. 537-541, May 2011.

[22]A. Recchia, A. Monti Guarnieri,A. Broquetas and J. Ruiz-Rodon, "Assessment of atmospheric phase screen impact on geosynchronous SAR," in *Proc. IGARSS*, Jul. 13-18, 2014, pp. 2243-2256.

[23]S. Hobbs, C. Mitchell, B. Forte, R. Holley, B. Snapir and P. Whittakker, "System Design for Geosynchronous Synthetic Aperture Radar Missions," *IEEE Geosci. Remote Sens*., vol. 52, no. 12, pp. 7750-7763, Dec. 2014.

[24]D. Bruno and S. E.Hobbs, "Radar imaging from geosynchronous orbit: Temporal decorrelation aspects," *IEEE Geosci. Remote Sens*., vol. 48, no. 7, pp. 506-520, Mar. 2001.

[25]D. Bruno and S. E. Hobbs, "Radar imaging from geosynchronous orbit: Temporal decorrelation aspects," *IEEE Trans. Geosci. Remote Sens.*, vol. 48, no. 7, pp. 2924-2929, Jul. 2010.

[26]S. Hobbs *et al.*, "Simulation of geosynchronous radar and atmospheric phase compensation constraints," in *Proc. IET Int. Radar Conf.*, Xi'an, China, 2013, pp. 1-6.

[27]J. Ruiz-Rodon, A. Broquetas, E. Makhoul,A. M. Guarnier and F. Rocca, " Nearly Zero Inclination Geosynchronous SAR Mission Analysis with Long Integration Time for Earth Observation," *IEEE Trans. Geosic. Remote Sens.*, vol. 52, no. 10, pp. 6379-6391, Oct. 2014.

[28]E. Makhoul, A. Broquetas, J. R. Rodon et al, "A Performance Evaluation of SAR-GMTI Missions for Maritime Applications," *IEEE Trans. Geosci. Remote Sens.*, vol. 53, no. 5, pp. 2496-2509, May. 2015.

[29]A. M. Guarnieri, A. Broquetas, A. Recchia, R. Fabio and R.-R. J, "Advanced Radar Geosynchronous Observation Systm:ARGOS," *IEEE Trans. Geosci. Remote Sens. Lett.*, vol. 12, no. 7, pp. 1406-11410, Jun. 2015.

[30]A. Recchia,A. M. Guarnieri and M. Belotti, "Demonstrative Geosynchronous SAR Products Affected by Clutter and APS Decorrelation," in *Proc. IEEE IGARSS*, 2015, pp: 1265-1268.

[31]M. E. Davis, J. J, Reis, "Operation of Geo SAR Foliage Penetration Modes in Spectrum Regulated Environment," in *IEEE Radar Conf.*, 2015, pp: 521-526.

[32]H. M. Braun, H. Baessler, C. Jonas, "Daily Monitoring of the Mediterranean Sea by Geosynchronous SAR," in *IEEE Radar Conf.*, 2016, pp: 1-4.

[33]H. Xu, L. Huang, X. Qiu, et al. "A New Geosynchronous SAR Constellation and Its Signal Characteristics and Its Signal Characteristics." *IEEE Aceess,* vol. 7, pp. 101539-101551, Aug. 2019.

[34]C. Hu, Z. Chen, X. Dong, and C. Cui, "Multistatic Geosynchronous SAR Resolution Analysis and Grating Lobe Suppression Based on Array Spatial Ambiguity Function," *IEEE Transactions on*

Geoscience and Remote Sensing, vol. 58, no. 9, pp. 6020-6038, 2020.

[35]C. Hu, Z. Chen, Y. Li, X. Dong, and S. Hobbs, "Research progress on geosynchronous synthetic aperture radar," *Fundamental Research*, vol. 1, no. 3, pp. 346-363, 2021.

[36]Z. Chen, C. Hu, X. Dong, Y. Li, W. Tian, and S. Hobbs, "Coherence-Based Geosynchronous SAR Tomography Employing Formation Flying: System Design and Performance Analysis," *IEEE Transactions on Geoscience and Remote Sensing*, vol. 59, no. 9, pp. 7165-7179, 2021.

[37]B. Zhou, X. Qi, H. Zhang. "An Accurate GEO SAR Range Model for Ultralong Integration Time Based on mth-Order Taylor Expansion." *Remote Sens.*, 13.2(2021):255.

[38]F. Chang, D. Li, Z. Dong, et al. "Elevation Spatial Variation Analysis and Compensation in GEO SAR Imaging." *Remote Sens.,* 13.10(2021): 1888.

[39]G-CLASS Hydroterra: An Earth Explorer Mission for Water Cycle Science. Accessed: Feb. 2019. [Online]. Available: https: //www. nceo.ac.uk/wp-content/uploads/2019/09/Stephen-HobbsG-CLASS-Hydroterra.pdf

[40]The European Space Agency (ESA). Call for New Earth Explorer Mission Ideas. Accessed: Sep. 2019. [Online]. Available: http: // www. esa. int/Our Activities/ Observing the Earth/ Call for new Earth Explorer mission ideas.

[41]The European Space Agency (ESA). Three Earth Explorer ideas selected. Accessed: Sep. 2019. [Online]. Available: http: //www. esa. int/Our_Activities/Observing the Earth/ Three Earth Explorer ideas selected.

[42]C. Li and M. He, "A Generalized Chirp-Scaling Algorithm for Geosynchronous Orbit SAR Staring Observations," *Sens.*, vol. 17, no. 5, pp. 1058, 2017.

[43]T. Zhang Z. Ding W. Tian T. Zeng and W. Yin "A 2-D nonlinear chirp scaling algorithm for high squint GEO SAR imaging based on optimal azimuth polynomial compensation" *IEEE J. Sel. Topics Appl. Earth Observ. Remote Sens.* vol. 10 no. 12 pp. 5724-5735 Dec. 2017.

[44]C. Li and M. He, "Technology of Pulse Repetition Frequency Variation for Geosynchronous Orbit SAR with Staring Imaging," *J. Univ. Electron. Sci. Tech. China*, vol 46, no. 6, pp. 917-922, Nov. 2016.

[45]C. Li and M. He, "Study on Azimuth Ambiguity for Geosynchronous Earth Orbit SAR," *J. Sign. Process.*, vol. 31, no. 6, pp. 694-701, Jun. 2015.

[46]T. Zhang et al., "The first helicopter platform-based equivalent GEO SAR experiment with long integration time", *IEEE Trans. Geosci. Remote Sens.*, vol. 58, no. 12, pp. 8518-8530, Dec. 2020.

[47]Z. Ding B. Shu W. Yin T. Zeng and T. Long "A modified frequency domain algorithm based on optimal azimuth quadratic factor compensation for geosynchronous SAR imaging" *IEEE J. Sel. Topics Appl. Earth Observ. Remote Sens.* vol. 9 no. 3 pp. 1119-1131 Mar. 2016.

[48]I. G. Cumming and F. H. Wong, *Digital Processing of Synthetic aperture Radar Data: Algorithms and Implementation,* vol. 4, no. 5, MA, USA: Artech House, 2005.

[49]Y. Gao, C. Hu, X. Dong and T. Long, "Accurate system parameter calculation and coverage analysis in GEO SAR", Proc. 9th EUSAR, pp. 607-610, Apr. 2012.

[50]J. C. Curlander, R .N. Mcdonough. "Synthetic Aperture Radar: Systems and Signal Processing".*Wiley*, 1991..

[51]C. Li and M. He, "Timing design for geosynchronous SAR ， " *Electron. Lett.*, vol. 52, no. 10, pp. 868-870, Oct. 2016.

[52]L. Huang, X. Qiu, D. Hu and C. Ding, "Focusing of Medium-Earth-Orbit SAR with Advanced Nonlinear Chirp Scaling Algotithm," *IEEE Geosci. Remote Sens.*, vol. 49, no. 1, pp. 500-509, Jan. 2011.

[53]C. Hu and T. Long, "The Accurate Focusing and Resolution Analysis Method in Geosynchronous SAR," *IEEE Geosci. Remote Sens.*, vol. 49, no. 10, pp. 3548-3564, Jan. 2011.

[54]G. Sun, M. Xing, Y. Wang, "A 2-D space-variant chirp scaling algorithm based on the RCM equalization and subband synthesis to process geosynchronous SAR data," *IEEE Geosci. Remote Sens.*, vol. 52, no. 8, pp. 4868-4880, Aug. 2014.

[55]M. Bao, M. Xing, Y. li. "Chirp Scaling Algorithm for GEO SAR Based on Fourth-order Range Equation," *Electron. Lett.*, vol. 48, no. 1, pp. 41-42, 2012.

[56]Z. Sun，J. Wu，J. Yang，Y. Huang，C. Li，D. Li, "Path Planning for GEO-UAV Bistatic SAR Using Constrained Adaptive Multiobjective Differential Evolution," IEEE Geosci. Remote Sens., vol. 54, no. 11, pp. 6444-6457, Oct. 2016.

Caipin Li was born in FuJian in China. He received the Bachelor's degree in computer science and technology from Air Force Engineering University, Xi'an, China, in 2007 and the M.S. degree in communication and information systems from the China Academy of Space Technology, Beijing, China, in 2010. From 2010 till now, he joined in the China Academy of Space Technology.He is currently a Professor of Satellite Payloads Engineering in the China Academy of Space Technology, Xi'an, China. He has published around forty papers, and applied over thirty patents. His research interests include spaceborne radar systems, new radar system design and SAR imaging processing.

Qingjun Zhang was born in Xuzhou, Jiangsu, China, in 1969. He received the Ph.D. degree from the Huazhong University of Science and Technology, Wuhan, China, in 2004., He is currently a Professor of Satellite Engineering with the China Academy of Space Technology (CAST), Beijing, China. He is also the Program Manager and the Chief Engineer of GF-3 and HY-2 programs, and the Chief Engineer of China – Brazil Earth Remote Sensing Satellite. He is also involved in the research of microwave remote sensing, especially in the synthetic aperture radar.,Dr. Zhang is a member of Technical Committee with CAST.

Jiao Liu was born in Xianyang, China, in 1989. She received the M.S. degree in communication and information systems from the China Academy of Space Technology, Xi'an, China, in 2014, and after that she joined the Payload System Innovation Center, Xi'an Branch of China Academy of Space Technology, Xi'an, China. Her research interests include satellite system design and SAR imaging processing.

Guoqiang Han was born in Xi'an, China. He received Bachelor's degree in machine design from Nanchang University, Nanchang, China, in 2008 and the master's degree in project management from Xi'an University of Electronic Science and Technology, Xi'an, China, in 2015.

From 2008 till now, he worked as a project manager in the Xi'an Institute of Space Radio Technology of Satellite remote sensing project management.

Bo Liu was born in Xianfeng, Hubei, China, in 1963. he received Bachelor's degree in majoring in Microwave Technology from the Radar Engineering Department of Northwest Telecommunications Engineering College, Xi'an, China, in 1982 and the master's degree in Electromagnetic Field and Microwave Technology from the China Academy of Space Technology(Xi'an), Xi'an, China, in 1990.

He is currently a Professor with the China Academy of Space Technology, Xi'an, China. His research areas include onboard antennas and microwave systems, navigation, and microwave remote sensing satellite payloads.

Chongdi Duan received the B.S. degree from the Harbin Institute of Technology, Harbin, China, in 1994, and the M.S. degree from the School of Electronic Engineering, Xidian University, Xi' an, China, in 2005. He received the Ph.D. degree with the School of Beijing Institute of Technology, Beijing, China,in 2022.

He is currently a Professor with the National Key Laboratory of Science and Technology on Space Microwave, China Academy of Space Technology. His research interests include radar signal waveform design, adaptive and array signal processing, mobile target detection, and high-speed real-time signal processors.

Zheng Lu (S'11–M'13–SM'19) received the B.S. degree in information engineering and the Ph.D. degree in target detection and recognition from the Beijing Institute of Technology, Beijing, China, in 2008 and 2013, respectively.

He is currently a Senior Engineer with Institute of Remote Sensing Satellite (IRSS), China Academy of Space Technology (CAST). His research interests include spaceborne radar systems and signal processing (particularly synthetic aperture radar and pulse Doppler radar). In these research fields, he is also the Principal Investigator and important participant of more than 20 grants and funding from different National or Governmental sources, including the National Natural Science Foundation of China (NSFC), the Management Office of Major Project of High-Resolution Earth Observation System, Beijing Municipal Science and Technology Commission, and Administrative Commission of Zhongguancun Science Park.